Environmental Science Processes & Impacts

ROYAL SOCIETY OF CHEMISTRY

PAPER

View Article Online
View Journal

Cite this: DOI: 10.1039/d5em00987a

Indoor air quality during cooking and cleaning: a modelling case study in a residential kitchen evaluated with real-world reference instrument measurements

Yizhou Su,[a] Roberto Sommariva,[a] James Levine,[ab] W. Joe F. Acton,[a] Ravi Sahu,[ac] James Brean,[a] William J. Bloss,[a] Andrea Mazzeo,[ad] Zaheer A. Nasir,[e] David R. Shaw,[fg] Zongbo Shi,[a] Jim R. Hopkins[gh] and Christian Pfrang *[ai]

Indoor air pollution during cooking and cleaning is influenced by complex interactions between direct emissions, ventilation-driven outdoor/indoor exchange, deposition and chemical reactions on surfaces, and indoor chemical processing. This study developed a flexible indoor single-box model (SBM-Flex) based on the INCHEM-Py indoor chemistry model to improve the representation of indoor chemistry and pollutant dynamics. The model contains chemical mechanisms of differing complexities, which can be chosen to balance computational efficiency and accuracy for specific applications. SBM-Flex was evaluated against a new observational dataset collected with reference instruments in a residential kitchen to evaluate the model's ability to simulate real-world conditions. The model qualitatively and quantitatively reproduces background conditions and episodic emission events, particularly for NO_x, CO, and monoterpenes. We showed that a revised HONO formation scheme, incorporating relative humidity dependence, improves the process-level representation of indoor radical chemistry, resulting in a more realistic HONO, OH and HO_2 description compared to a static HONO treatment. Simulated cooking and cleaning events highlight the importance of event-specific emissions and occupant-related effects, particularly enhanced surface deposition due to human presence, which influences O_3 removal. Comparison between measurement-informed and inventory-based emissions reveals significant discrepancies, with inventory emissions often, though not uniformly, higher than real-world values. These findings underscore the need for activity-specific emission inventories and improved ventilation representation. SBM-Flex offers a promising approach for indoor air quality modelling providing valuable insights into the key processes that govern pollutant behaviour in residential environments and hence identifying priorities to reduce exposure and protect health.

Received 28th November 2025
Accepted 23rd April 2026

DOI: 10.1039/d5em00987a

rsc.li/espi

Environmental significance

We present a model that improves indoor air chemistry modelling and allows for tailored complexity of chemical mechanisms; this model is evaluated against unique reference data collected during cooking and cleaning in a kitchen in a real, lived in home in the UK. We demonstrate that the relative-humidity dependent HONO scheme provides more realistic predictions of OH and HO_2 levels. We quantify how event-specific emissions and occupant presence alter ozone removal *via* surfaces and show that the observed emissions in real homes can diverge massively from values used in indoor inventories, illustrating that activity-specific data in a wide range of settings are urgently needed.

[a]*School of Geography, Earth and Environmental Sciences, University of Birmingham, Edgbaston, B15 2TT, Birmingham, UK. E-mail: c.pfrang@bham.ac.uk*

[b]*Cambridge Zero, University of Cambridge, The Old Schools, Trinity Lane, Cambridge, CB2 1TN, UK*

[c]*International Centre for Integrated Mountain Development (ICIMOD), Khumaltar, Lalitpur, G. P. O. Box 3226, Kathmandu, Nepal*

[d]*Lancaster Environment Centre (LEC), Lancaster University, Bailrigg Campus, Lancaster LA1 4YW, UK*

[e]*Faculty of Engineering and Applied Sciences, Cranfield Environment Centre, Cranfield University, College Road, Cranfield MK43 0AL, UK*

[f]*Department of Environment and Geography, University of York, York, YO10 5NG, UK*

[g]*National Centre for Atmospheric Science, Department of Chemistry, University of York, Heslington, York, YO10 5DD, UK*

[h]*Wolfson Atmospheric Chemistry Laboratories, University of York, York YO10 5DD, UK*

[i]*Department of Meteorology, University of Reading, Whiteknights, Earley Gate, RG6 6BB, Reading, UK*

1 Introduction

Indoor air quality (IAQ) plays a crucial role in human health and well-being, as people spend approximately 90% of their time indoors, with residential spaces being the primary microenvironment.[1–3] While outdoor air pollution has been extensively studied, indoor air remains less well-characterized despite its potential for greater human exposure. Unlike outdoor environments, where atmospheric dilution, chemical processing, and precipitation effectively reduce pollutant levels, indoor air quality is shaped by a complex interplay of emissions, ventilation, surface interactions, and human activities, leading to a greater propensity for pollutant accumulation.[4–6] As a result, pollutant concentrations indoors are often twice as high as those outdoors, leading to prolonged exposure and potential health risks.[7] However, the degree of indoor enrichment varies strongly by chemical species.[8] Pollutants dominated by outdoor infiltration and subject to efficient indoor removal, such as ozone, are typically lower indoors or show indoor-to-outdoor (I/O) ratios close to one.[6] In contrast, species with strong indoor sources, including nitrogen oxides and volatile organic compounds, are frequently enriched indoors.[8,9] Reported I/O ratios can exceed 2–10 for compounds associated with episodic indoor emissions.[8,10]

Among indoor activities, cooking and cleaning are key episodic sources of air pollution, releasing a diverse array of gaseous species—including nitrogen oxides (NO_x), carbon monoxide (CO), and volatile organic compounds (VOCs)—as well as fine particulate matter ($PM_{2.5}$).[11–17] These emissions not only elevate indoor pollutant concentrations but also drive secondary chemistry, leading to the formation of secondary organic aerosols (SOA) and other oxidation products.[18] Exposure to these pollutants has been associated with adverse health effects, including respiratory and cardiovascular diseases,[19] making it essential to understand their behaviour in indoor environments. Given the frequent occurrence of these emission events in households, accurately characterizing their impact on indoor chemical processes is crucial for a better understanding the transformation and fate of indoor air pollutants, exposure assessment and the development of effective mitigation strategies.

Understanding indoor air chemistry requires a comprehensive yet targeted approach to pollutant selection, particularly in environments influenced by episodic emissions such as cooking and cleaning. These activities release a complex mixture of gases and aerosols, including both primary emissions and reactive species that contribute to secondary transformations.[11,20] Among these, CO, NO, and NO_2 serve as key tracers of combustion processes and are widely recognized as indicators of gas stove emissions.[21] Monoterpenes, especially limonene, originate from both food preparation and fragranced cleaning products, highlighting their dual role in indoor emissions.[22–24] In addition to these directly emitted compounds, various VOCs, including oxygenated and aromatic species, are commonly present in indoor air due to emissions from cooking, cleaning, combustion, and off-gassing from household products and materials. These compounds play a crucial role in indoor photochemistry and SOA formation.[25,26] Investigating the emissions and transformation of these species is crucial for assessing the oxidative capacity of indoor environments, the formation of secondary pollutants, and potential human exposure risks in particular for vulnerable groups.[27,28] Given their importance, these species have been the focus of numerous indoor air studies, yet significant uncertainties remain regarding their activity-induced variations during real-world activities such as cooking and cleaning.[7]

Beyond the direct emissions of pollutants, the oxidative capacity of indoor air determines their transformation and removal, influencing both secondary chemistry and human exposure. In indoor environments, this oxidative capacity is strongly modulated by nitrous acid (HONO), which is widely recognised as a major source of OH radicals indoors, particularly under typical residential lighting conditions.[29] Oxidation reactions in outdoor environments are dominated by O_3, NO_3 and OH radicals. Alongside these, indoor oxidation is strongly influenced by heterogeneous reactions, surface deposition, and human activity.[30] Among the key oxidants, OH plays a central role in VOC degradation and secondary product formation: its production indoors relies heavily on photolysis of nitrous acid, rather than O_3-driven photochemistry.[29,31] HONO is primarily formed through heterogeneous NO_2 hydrolysis on indoor surfaces, but its production efficiency depends strongly on relative humidity (RH), which regulates the competition between HONO and nitrate (NO_3^-) formation.[32] Cooking and cleaning activities significantly influence RH due to water vapour release, which dynamically alters surface chemistry and potentially affects indoor oxidation capacity *via* increased HONO production. However, indoor air quality models differ substantially in how they represent indoor HONO. For example, PyCHAM[33] uses a gas–wall partitioning framework to simulate surface uptake and release of gases, but does not explicitly model the heterogeneous formation of HONO. The HOMEChem[34] field campaign provided observational evidence for surface-mediated HONO production, particularly under elevated humidity conditions, though it did not include a quantitative mechanism for HONO formation. INCHEM-Py v1.2[35] has utilised a custom HONO surface mechanism to simulate dry and wet surface loss during cleaning activities during the HOMEChem campaign,[36] but the version 1.2 of the model only applies a fixed HONO emission rate, neglecting the variable influence of factors like RH and indoor activities.

Recent advancements in IAQ modelling have led to the development of various models, each addressing different aspects of indoor atmospheric processes. Chemical box models, such as INCHEM-Py and PyCHAM, have been widely used to simulate indoor gas-phase chemistry, surface interactions, and indoor–outdoor exchange.[33,35] INCHEM-Py provides a comprehensive representation of indoor chemical and physical processes and is available as open source;[37] however, its single-mechanism structure limits flexibility, making it computationally demanding when modelling complex environments such as entire buildings. More dynamically advanced modelling approaches, including computational fluid dynamics (CFD;

most recent example coupling CFD with indoor chemistry is ChemFlow3D – see 38 and multiphase kinetic modelling, can represent high-resolution spatial and temporal variability. These models offer detailed representations of spatial and temporal variations in pollutant distributions but the reduced mechanisms they use to maintain computational efficiency are still evaluated by complex chemical models such as INCHEM-Py.[39] Such models are highly resource-intensive and often impractical for routine IAQ assessments.

A key challenge in IAQ modelling remains the balance between chemical complexity and computational efficiency. Many models employ highly detailed mechanisms, such as the Master Chemical Mechanism (MCM),[40,41] to explicitly capture VOC oxidation pathways. However, their computational demands are substantial, making them impractical for simulations beyond 0D well-mixed environments or over extended time periods. Another key challenge is that static emission inventories[42] commonly used in IAQ models generalize emission factors across diverse indoor environments and activities.[43] While useful for long-term exposure assessments, these inventories often fail to capture short-term, event-driven emissions that are highly variable in real-world scenarios, such as cooking and cleaning; the consequences for indoor air quality of higher rates of emission for shorter periods of time may differ markedly from those of lower, time-averaged emissions employed over a longer period. Current IAQ models would benefit from incorporating adaptable chemical mechanisms and real-time emission estimates, allowing for improved prediction of indoor pollution events without excessive computational costs.

To address these gaps, we developed SBM-Flex, an optimised indoor air quality model derived from INCHEM-Py, which incorporates flexible chemical mechanisms and a revised parameterization of humidity-dependent HONO formation. This study systematically evaluates SBM-Flex's ability to simulate pollutant dynamics in a real residential kitchen, capturing both primary emissions and secondary transformations. By comparing different chemical mechanisms and assessing the impact of event-specific emissions and human presence, we provide a quantitative assessment of the trade-offs between chemical complexity, computational efficiency, and model accuracy. Furthermore, by benchmarking inferred emission rates against established indoor emission inventories, this study evaluates the representativeness of current emission factor estimates in real-world cooking and cleaning scenarios. This study advances the representation of episodic indoor air chemistry by integrating flexible chemical mechanisms with event-driven emissions, providing a framework for improving predictive accuracy in indoor air quality modelling.

2 Methodology

2.1 Indoor and outdoor measurements in a residential kitchen

Reference-grade air quality measurements for both indoor and outdoor environments were conducted in the kitchen of a suburban house in the West Midlands, United Kingdom, during August 2023. This study focusses specifically on the impact of kitchen-related activities, including human presence, cooking, and cleaning, on indoor air quality on 17th August 2023.

The layout of the kitchen is shown in Fig. 1. The kitchen is equipped with a gas hob for cooking and features a door adjacent to a window positioned above the sink, which provides ventilation to the outside. The kitchen has dimensions of 4.80 $\times$ 2.70 $\times$ 2.40 m, with surfaces composed of different materials: the walls and ceiling are painted, the floor is covered with tiles, and the cabinets are made of wood that has not been recently painted or refinished. Additional materials include glass (windows and table), metal (sink), and plastic (worktop). The key characteristics of this kitchen, including the effective surface area and volume (excluding the volume occupied by the sink and cabinets), surface material distribution, lighting type, and glass type, are summarised in Table S1.

A suite of reference instruments was deployed to measure a wide range of gas-phase species as well as the mass concentration of particulate matter. These instruments form part of UK's Air-Quality Supersite Triplet (UK-AQST). All gas-phase instruments were deployed in the adjacent garage near the kitchen (see Fig. 1). Sampling was performed through two dedicated inlets, one for indoor air and one for outdoor air. A custom-developed auto-valve switched between indoor and outdoor sampling every 30 minutes to avoid impacting indoor conditions due to the continuous removal of significant volumes of indoor air needed for the large suite of reference instruments. This design enables near-simultaneous monitoring of indoor and outdoor air pollutants with a single set of instruments, without compromising the representativeness of the indoor environment. The 30-minutes switching interval was selected based on instrument response times, required air flow rates, expected temporal variability of pollutant concentrations, and the need to ensure that the collected data adequately reflect hourly conditions. To minimise the influence of residual pollutants in the inlet line during the transition between indoor and outdoor sampling, as well as potential delays in pollutant transport through the inlet, data were discarded across the switching period. Only the middle 20 minutes of each sampling period were retained, as these points consistently reflected stable concentrations based on instrument response characteristics and preliminary testing. This approach ensured that

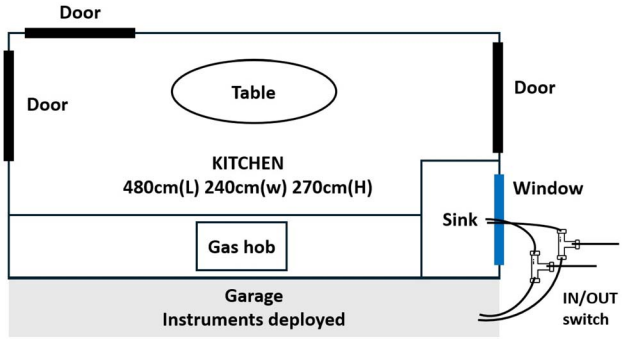

Fig. 1 Schematic representation of the kitchen layout used in this study.

the analysed data were unaffected by transient effects and were representative of the target sampling environment.

The total flow rate for the gas-phase instruments was 4 L min^{-1}. The indoor inlet extended through the window above the sink, with a sampling height of 1.7–1.8 m, while the outdoor inlet sampled ambient air from the surrounding environment. Carbon monoxide (CO) concentrations were measured using the Thermo Scientific™ 48iQ Carbon Monoxide Analyser, with a 5-minutes time resolution; and ozone (O_3) using the Thermo Scientific™ 49i Ozone Analyser, with a 1-minutes time resolution; while nitric oxide (NO) and nitrogen dioxide (NO_2) using the Thermo Scientific™ 42iQ NO–NO_2-NO_x Analyser, with a 1-minute time resolution.

Ambient temperature, pressure, relative humidity, and particulate matter mass concentrations were monitored using two Palas Fidas® 200 E instruments. One was permanently housed inside, and one was permanently housed outside. The outdoor instrument was housed alongside the gas-phase instruments, while the indoor instrument was placed in the room adjacent to the kitchen. Particulate matter was sampled continuously in both environments, with a 1-min time resolution. Both instruments have a flowrate of 4.8 L min^{-1}. Together with the gas-phase sampling flow (4.0 L min^{-1}), this corresponds to a total sampling flow of 8.8 L min^{-1}, equivalent to approximately 1% of the kitchen volume (24.52 m^3) over a 30-minutes sampling period, indicating that the potential impact of the sampling system on indoor conditions was minimal.

VOCs were measured using an IONICON PTR-ToF-MS 1000 – trace VOC Analyser, which enables real-time, high-sensitivity detection of individual VOC species based on their mass-to-charge ratios (m/z), with a time resolution of 1 second. Specific VOCs identified in this study include methanol (CH_3OH), acetaldehyde (CH_3CHO), formic acid (HCOOH), acetone (CH_3COCH_3), isoprene (C_5H_8), benzene, toluene, xylenes, trimethylbenzenes, and monoterpenes. These compounds were selected due to their established relevance to indoor air chemistry and cooking-related emissions, as well as their inclusion in the UK's Indoor Air Quality Guidelines for selected Volatile Organic Compounds (VOCs), which highlights their regulatory and health significance.[44] VOC mixing ratios are reported in parts per billion (ppb). The PTR-ToF-MS shared an inlet with the other gas-phase analysers, and the inlet flow was set to 50 mL min^{-1}. The PTR-ToF-MS was operated with an E/N ratio of 121 Td (where E is the electric field strength and N is the buffer gas density). The instrument was calibrated off site about 4 months before and after the measurement campaign using a multi component gas standard (Apel-Riemer Environmental, Miami). The sensitivity for each mass was then calculated using a transmission curve as described by Taipale *et al.*[45]

To assess the uncertainty in VOC quantification, outdoor VOC mixing ratios measured at the experimental house were compared with those recorded at the Birmingham Air Quality Supersite (BAQS), an established urban background air quality monitoring site located 11.2 km away. VOCs at BAQS were measured using GC-MS as described by Li *et al.*[46] As the instrument was not calibrated on site, instrumental sensitivity may have varied over the deployment period. The inter-site comparison therefore provides a more representative estimate of uncertainty under field conditions. Given the expected variability across the urban area, this comparison showed good agreement, with average mixing ratios at the experimental house ranging from 25–250% of those recorded at BAQS (Fig. S6).

During the measurement period, time-activity diaries were kept, and the inhabitants of the private dwelling were asked to log their activities, including the timing of cooking and cleaning, as well as their presence in the kitchen, to facilitate interpretation of the measurements and of the model results.

2.2 The single-box-flexible model (SBM-Flex)

The single-box-flexible model (SBM-Flex) has been developed to simulate indoor air quality in buildings of varying complexity and design. It extends the widely used INCHEM-Py indoor chemistry box-model,[35,47] which represents a single room, incorporating air exchange between indoor and outdoor environments. SBM-Flex includes the option to linking multiple instances of the model, thus enabling the simulation of complex indoor air quality dynamics across interconnected spaces in a multi-box set-up. Here we present the first application of SBM-Flex, in single-box mode, for evaluation using single-room reference instrument field measurements.

SBM-Flex is based on the latest version of INCHEM-Py (v1.2).[35] This version incorporates the Master Chemical Mechanism Version 3.3.1 (MCM v3.3.1),[40,41] with additional gas-phase chemistry (referred to as "INCHEM chemistry module" in the rest of the paper) specific to indoor environments, including biogenic and oxygenated volatile organic compounds (BVOCs, OVOCs), and chlorine chemistry. The model accounts for photolysis rate corrections under indoor lighting conditions and attenuated outdoor light, gas-particle partitioning, and explicitly treats indoor emissions and deposition of gas-phase species and particles. Additionally, indoor–outdoor air exchange is incorporated into the model framework.

Building on this foundation, several modifications were introduced in the development of SBM-Flex to enhance computational efficiency and improve the representation of key processes in indoor air chemistry. These modifications include:

2.2.1 Multiple chemical mechanism options. SBM-Flex provides flexibility in chemical complexity by incorporating the following four different chemical mechanisms:

- Full mechanism: uses the complete MCM v3.3.1, consisting of 5833 species, coupled with the INCHEM chemistry module and gas-to-particle partitioning. This mechanism provides the highest level of chemical detail but is computationally intensive, and is the same mechanism used in INCHEM-Py v1.2.
- Subset mechanism: a subset of the MCM, containing 2575 species, optimised to balance computational efficiency and chemical accuracy. Selected species were chosen based on their roles in SOA formation, radical chemistry, and human health impacts, guided by the Indoor Emissions Inventory.[42] While computationally efficient, it retains the INCHEM chemistry modules and gas-to-particle partitioning to preserve key indoor oxidation and aerosol processes.

• Reduced mechanism: a highly streamlined Reduced Chemical Scheme (RCS), developed as an alternative to the full MCM or its subset version. Based on,[48] this mechanism consists of 51 species and 136 reactions, incorporating up-to-date chemical kinetics parameters and simplified NO_3 and Cl radical chemistry. It includes the INCHEM chemistry modules and is particularly suitable for large-scale simulations where computational efficiency is a priority.

• Mini mechanism: a simplified version of the RCS, using the same 51 species, but without the INCHEM chemistry module, designed for testing and model development.

2.2.2 Implementation of a humidity-dependent HONO parameterisation

To improve the representation of indoor heterogeneous chemistry, a humidity-dependent parameterization was introduced for HONO emissions from NO_2 reactions on indoor surfaces. The following surface reaction was implemented to represent HONO formation from NO_2:

$$2NO_2\ (surf) + H_2O \rightarrow HONO + HNO_3$$

Rate constant: $k = 8.0 \times 10^{-20}$ cm^3 molecule^{-1} s^{-1} (ref. 32)

This RH-dependent parameterisation provides a more physically realistic representation of surface HONO formation by coupling HONO yields to surface water availability; its impact is evaluated below.

2.2.3 Room occupancy and hourly variability of environmental conditions. SBM-Flex builds on existing INCHEM-Py v1.2 capabilities, such as surface deposition dependent on the surface-to-volume ratio, breath emissions from humans (adults ≥10 years old; children <10 years old), and hourly variations in Air Change Rate (ACR) and indoor lighting, by adding two further elements: hourly variations in relative humidity (RH) and in the number of adult and child occupants. These parameters are specified through an input file, enabling direct incorporation of occupant numbers, hourly humidity levels, air change rates, and lighting schedules, thereby enhancing the model's dynamic representation of indoor air chemistry.

2.3 Model setup

The SBM-Flex model described in the previous section was applied to simulate indoor air quality in the residential kitchen on 17 August 2023, a day selected due to clear evidence of cooking and cleaning activities based on the occupants' logs and *in situ* measurements.

To assess indoor air quality, 15 air pollutants were selected for the simulation. These species represent a combination of regulated air pollutants (O_3, NO_2, CO, $PM_{2.5}$), direct emission from cooking process by using gas stove (NO); and key reactive VOCs spanning a range of typical indoor sources, including emissions from cooking, building materials, cleaning products, and secondary chemical formation. These VOCs include methanol, acetaldehyde, formic acid, acetone, isoprene, benzene, toluene, xylenes, trimethylbenzenes, and monoterpenes.

For xylenes, trimethylbenzenes, and monoterpenes, the PTR-ToF-MS provided only bulk signal intensities at the corresponding *m*/*z* values, without resolving individual isomers or isobaric compounds. This is a recognised limitation of real-time mass spectrometric techniques applied to complex VOC mixtures.[49,50] To allow chemical mechanism modelling, these bulk signals were disaggregated into individual species based on the species structure defined in the Master Chemical Mechanism (MCM v3.3.1). Prior to disaggregation, it was assumed that each *m*/*z* signal originated exclusively from structural isomers within the same compound class, excluding other isobaric compounds. Each species within these groups was assumed to contribute equally to the measured total concentration, consistent with the use of lumped VOC representations commonly adopted when real-time mass spectrometric measurements do not resolve individual isomers and when the modelling focus is on bulk oxidative chemistry rather than compound-specific products.[51,52] Specifically, xylenes were split equally into *o*-xylene (OXYL), m-xylene (MXYL), and *p*-xylene (PXYL); trimethylbenzenes into 1,2,3-trimethylbenzene (TM123B), 1,2,4-trimethylbenzene (TM124B), and 1,3,5-trimethylbenzene (TM135B); and monoterpenes into α-pinene, β-pinene, limonene, carene, and camphene. While this equal-split assumption introduces some degree of uncertainty, it ensures consistency with the mechanism structure used in SBM-Flex and provides a practical solution in the absence of environment-specific isomer speciation data. This approach allows the bulk signal measurements to be used consistently within the mechanism, enabling the representation of overall chemical reactivity within the model framework.

The model was initialised using measured indoor and outdoor concentrations along with detailed physical parameters of the kitchen (see Table S1). These observational inputs were used to define realistic initial and boundary conditions for the case study, rather than to tune model parameters or optimise agreement with the measured time series. Indoor initial concentrations were set to the first hourly average measured inside the kitchen, providing a realistic starting point for simulating the temporal evolution of indoor chemistry. Outdoor concentrations were prescribed as fixed inputs to constrain the boundary conditions for indoor chemistry and were not dynamically updated based on indoor–outdoor exchange, consistent with the INCHEM chemistry module design. For O_3, NO, and NO_2, time-varying diurnal profiles were fitted to the hourly outdoor measurements acquired on 17 August (see Fig. S1) to capture photochemical influences and emission-driven variability. These profiles are critical for representing processes such as NO titration, HONO formation, and O_3-driven oxidation. For all other species, constant daily average concentrations were used to represent the most characteristic outdoor levels on that day.

The ACR was constrained by fitting modelled indoor concentrations of O_3, NO, NO_2, and CO, which, outside periods of direct indoor emissions, are expected to be dominated

primarily by ventilation-driven exchange with outdoor air. To minimise the influence of indoor sources such as cooking and cleaning, periods from 06:00 to 08:00 and from 15:00 to 18:00 were excluded based on the volunteer activity records.

Although O_3 undergoes indoor loss through deposition and NO_x may also be influenced by indoor photochemistry, these species were not treated as individually conservative tracers. Instead, ACR was evaluated consistently across multiple gas-phase species in order to reduce reliance on any single compound that may be affected by additional indoor processes. This assumption is supported by the behaviour of CO, which was associated with gas hob use and showed no notable indoor enhancement outside the excluded periods. The absence of elevated CO during the selected fitting window suggests that indoor combustion sources were effectively removed from the ACR evaluation period.

Candidate ACR values were compared using both model-observation diurnal profiles (Fig. S2) and root mean square error (RMSE) values for O_3, NO, NO_2, and CO during the non-emission hours (Table S2). The results indicate that the apparent optimum ACR depends to some extent on the gas used for comparison. O_3 showed the greatest sensitivity and favoured values around 7–8 h^{-1}, while NO_2 showed a weaker but still systematic improvement with increasing ACR. In contrast, NO varied only marginally across the tested range, and CO showed no sensitivity to ACR during the selected fitting period. The multi-species comparison therefore supported an intermediate ACR, rather than selection based on O3 alone.

To further examine this choice, an additional NO sensitivity analysis was performed for the midday period (Fig. S3), when differences between ACR scenarios became more visible. This diagnostic comparison showed that higher ACR values did not improve, and slightly worsened, the reproduction of midday NO behaviour. An ACR of 7 h^{-1} was therefore retained as the most balanced choice across species, rather than selecting a higher value solely on the basis of the minimum O_3 RMSE. This value is consistent with previous studies under window-open conditions,[53] and aligns with the activity log, which states that the kitchen window remained open throughout the day.

3 Results and discussion

This section evaluates the performance of SBM-Flex in reproducing observed indoor air composition during cooking and cleaning events, with a focus on the effects of chemical mechanism complexity and humidity-dependent surface HONO formation. By systematically comparing model predictions using different chemical mechanisms against measurements,

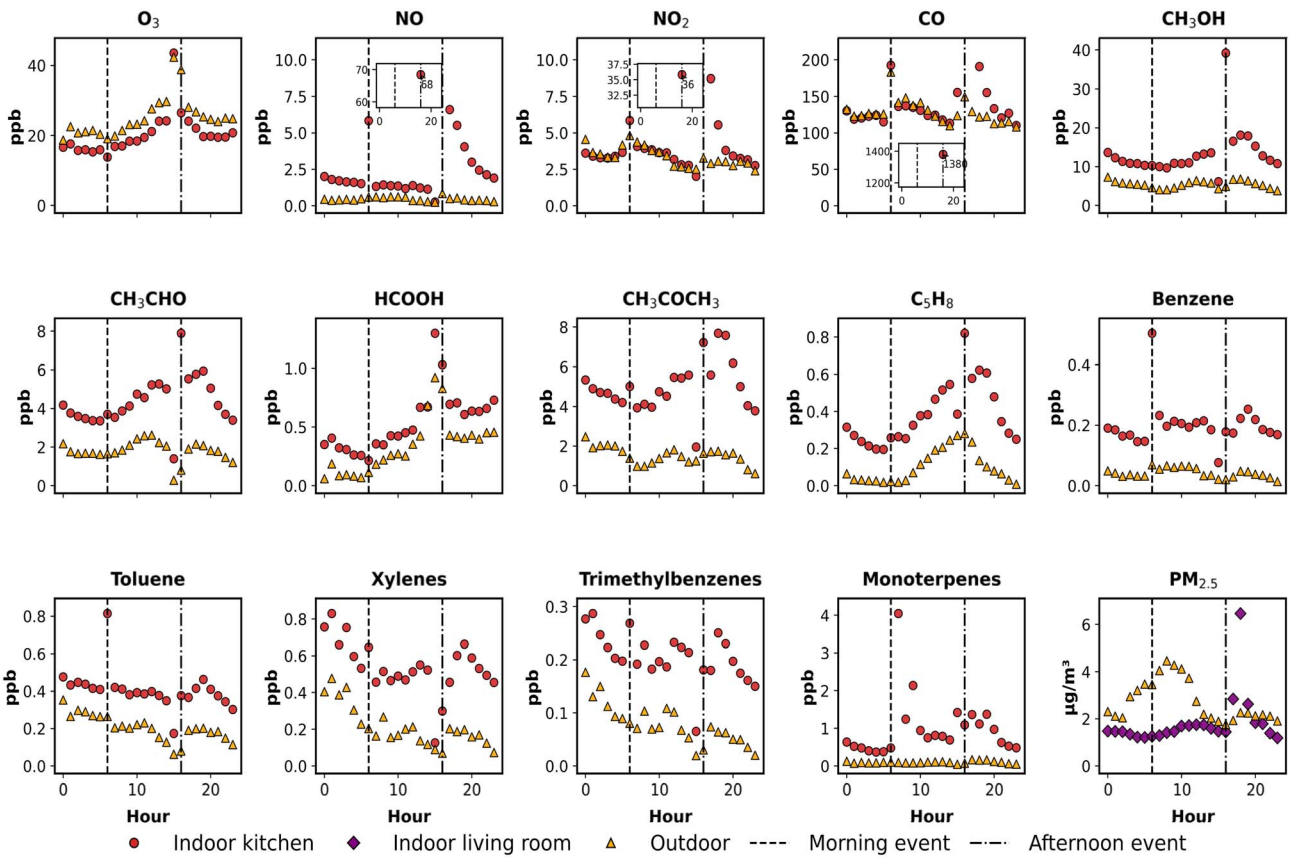

Fig. 2 Observed hourly indoor and outdoor mixing ratios/concentrations of 15 air pollutants on 17 August 2023. Morning and afternoon events are highlighted, corresponding to cooking and cleaning periods identified from volunteer activity logs. Inset subplots are included for NO, NO_2, and CO to illustrate their extreme peak values. ($PM_{2.5}$ was measured in the adjacent living room and is represented using a distinct colour and marker to differentiate it from kitchen-based measurements).

we assess the extent to which mechanism simplifications impact indoor air quality modelling accuracy. Additionally, inferred emission rates from SBM-Flex are compared with existing indoor emission inventories to examine their representativeness for real-world residential kitchens.

3.1 Observations of indoor and outdoor air quality

Fig. 2 presents the observed hourly profiles of indoor and outdoor concentrations for 15 air pollutants on 17 August 2023, capturing their diurnal variations throughout the day. The highlighted events correspond to cooking and cleaning periods identified from volunteer activity logs. Although results are shown as hourly means for clarity, the underlying measurements were collected at much higher temporal resolution and clearly resolve short-duration cooking and cleaning events; a comparison between native-resolution time series and hourly means for selected species is provided in the SI (Fig. S7). To better visualise species exhibiting extreme concentration peaks—specifically NO, NO_2, and CO for the afternoon event—inset subplots are incorporated within their respective panels. Indoor $PM_{2.5}$ was measured in the adjacent living room and is plotted using a distinct marker and colour to distinguish it from kitchen-based measurements. Outdoor species such as O_3, NO, and NO_2 exhibit characteristic diurnal cycles, reflecting the combined effects of local traffic emissions and photochemical activity. Morning and afternoon NO_x peaks correspond to rush-hour traffic, while the daytime peak in O_3 is driven by photochemical production and steady-state.[54,55]

Indoor pollutant concentrations broadly track these outdoor variations during non-cooking periods, highlighting the strong influence of ventilation-driven outdoor-to-indoor transport. This coupling is particularly evident for O_3, NO_x, and CO, providing independent observational support for the air change rate derived during model setup. The rapid decline in indoor CO concentrations shortly after cooking events further supports this rate, as it is consistent with a fast removal process under a high ventilation regime. Beyond these species, several VOCs, such as HCOOH, and CH_3CHO, also exhibit indoor profiles that follow outdoor trends during background periods, reinforcing the dominant role of ventilation in shaping indoor air quality when active emissions are absent. Under such high ventilation conditions, similar indoor–outdoor temporal variability combined with a persistent indoor concentration offset is consistent with ventilation-dominated transport superimposed on weak but continuous indoor sources, such as off-gassing from materials, surface re-emission, and human presence.

In contrast, distinct indoor peaks for other species appear during cooking and cleaning periods, as logged by the occupants, highlighting the dominant influence of indoor sources during these episodes. These peaks are most pronounced for NO, NO_2, and CO, with strong increases observed around 06:00 and 16:00, corresponding to cooking activities. The timing and magnitude of these peaks are consistent with primary emissions from gas combustion, in agreement with previous studies of cooking-related indoor air pollution.[9,21,34]

VOCs exhibited broader and more sustained indoor peaks compared to inorganic species, reflecting the influence of both primary emissions and secondary formation. Monoterpenes showed a sharp increase at 07:00, corresponding to cleaning activities following morning cooking, and a more pronounced rise between 15:00 and 17:00, corresponding to a sequence of food preparation, cooking, and subsequent cleaning, as recorded in the volunteer activity logs. These patterns suggest emissions from fragranced products, consistent with prior studies linking monoterpenes (*e.g.*, limonene) to cleaning agents and air fresheners.[56,57] Oxygenated VOCs such as CH_3OH, CH_3CHO, and HCOOH increased notably during the afternoon period, likely due to a combination of cooking emissions and subsequent indoor photochemical reactions.[29] Unlike primary pollutants that peaked sharply and then declined rapidly, these species remained elevated or declined only slowly following the event, suggesting continued production indoors. This behaviour is consistent with secondary formation from reactions involving ozone and reactive VOCs such as monoterpenes under indoor conditions.[47] CH_3COCH_3 displayed a prolonged afternoon elevation, which aligns with continuous occupancy in the kitchen and is likely attributable to breath emissions.[58] In contrast, aromatic VOCs (*e.g.*, benzene, toluene, xylenes, and trimethylbenzenes) showed relatively stable levels, with only moderate afternoon increases, suggesting contributions from background sources such as materials or residual infiltration.

Indoor $PM_{2.5}$ concentrations, measured in the adjacent living room, began to rise gradually after the cooking event (16:00–17:00), reaching a distinct peak shortly after 18:00 and then declining steadily. This post-event rise reflects the transport of particles emitted during cooking in the kitchen into the adjacent space. Minute-resolution data shown in Fig. S4 clearly show this rise-and-fall pattern, providing direct evidence of inter-room pollutant transfer. These observations indicate that emissions from specific indoor activities, such as cooking, can influence air quality in adjacent spaces through inter-room transport.

3.2 Effects of improved HONO formation on indoor chemistry

Accurate simulation of indoor oxidation chemistry requires realistic representation of surface HONO formation, as photolysis of HONO is a primary indoor source of OH radicals, driving VOC oxidation and secondary product formation. In INCHEM-Py version 1.2, on which SBM-Flex is based, surface HONO formation is parameterised using a simplified empirical expression,[47] which assumes all surface-adsorbed NO_2 is fully converted to HONO. This static treatment neglects the established dependence of HONO yields on relative humidity, which modulates the competition between HONO and HNO_3 formation.[30,59] This omission is particularly problematic in kitchens, where cooking and cleaning introduce large humidity fluctuations, dynamically altering surface water films and influencing NO_2 hydrolysis chemistry.

To address this, SBM-Flex implements a revised HONO formation scheme that explicitly couples HONO yields to surface RH, following,[32] as described in the previous section.

This dynamic treatment links surface chemistry to indoor environmental conditions, replacing the static emission factor with a process-based representation that explicitly captures the humidity dependence of HONO yields, providing a more physically grounded representation of surface HONO formation for indoor radical sources. The kitchen environment examined here, characterised by highly hygroscopic surfaces (painted walls, tiles) and persistently high relative humidity (RH consistently >60% throughout the day, see Fig. S8), provides a relevant real-world case for evaluating the implications of this improvement under typical residential humidity conditions.

Fig. 3 compares the simulated diurnal profiles of key photochemically active species and total OH reactivity, using SBM-Flex and INCHEM-Py, across the Full, Subset, and Reduced mechanisms. This comparison evaluates both the impact of the revised HONO parameterisation and the performance of mechanisms with varying levels of chemical complexity. Several important findings emerge from this comparison.

Across all mechanisms, SBM-Flex systematically predicts lower HONO concentrations than INCHEM-Py at all times of the day. This reduction reflects the revised treatment of surface HONO formation in SBM-Flex, where surface-processed NO_2 is partitioned between HONO and nitrate (NO_3^-) formation according to a relative-humidity-dependent parameterisation, rather than being assumed to convert entirely to HONO as in INCHEM-Py v1.2. The effect of lower HONO concentrations in SBM-Flex propagates through the entire oxidation system. Reduced HONO photolysis weakens the primary source of OH, leading to lower OH and HO_2 concentrations across the full diurnal cycle. This highlights the central role of surface-derived HONO in sustaining indoor radical chemistry. Both SBM-Flex and INCHEM-Py capture the expected daytime rise in OH and HO_2 due to photolysis-driven radical production, but SBM-Flex consistently maintains lower absolute levels, reflecting its reduced HONO source strength. While the revised parameterisation explicitly links HONO formation to RH *via* surface water availability, the baseline SBM-Flex simulation uses the observed indoor RH measured in the kitchen. To assess the sensitivity of this scheme to humidity, additional diagnostic simulations were performed using fixed low (10%) and high (90%) RH values, representing idealised bounds rather than realistic indoor conditions.

The resulting diurnal profiles of HONO, OH, and total OH reactivity are shown in Fig. S7. Across these simulations, HONO and OH concentrations exhibit only minor differences within the observed RH range. This limited sensitivity reflects the persistently high indoor humidity during the measurement period (RH was consistently >60%), under which surface water

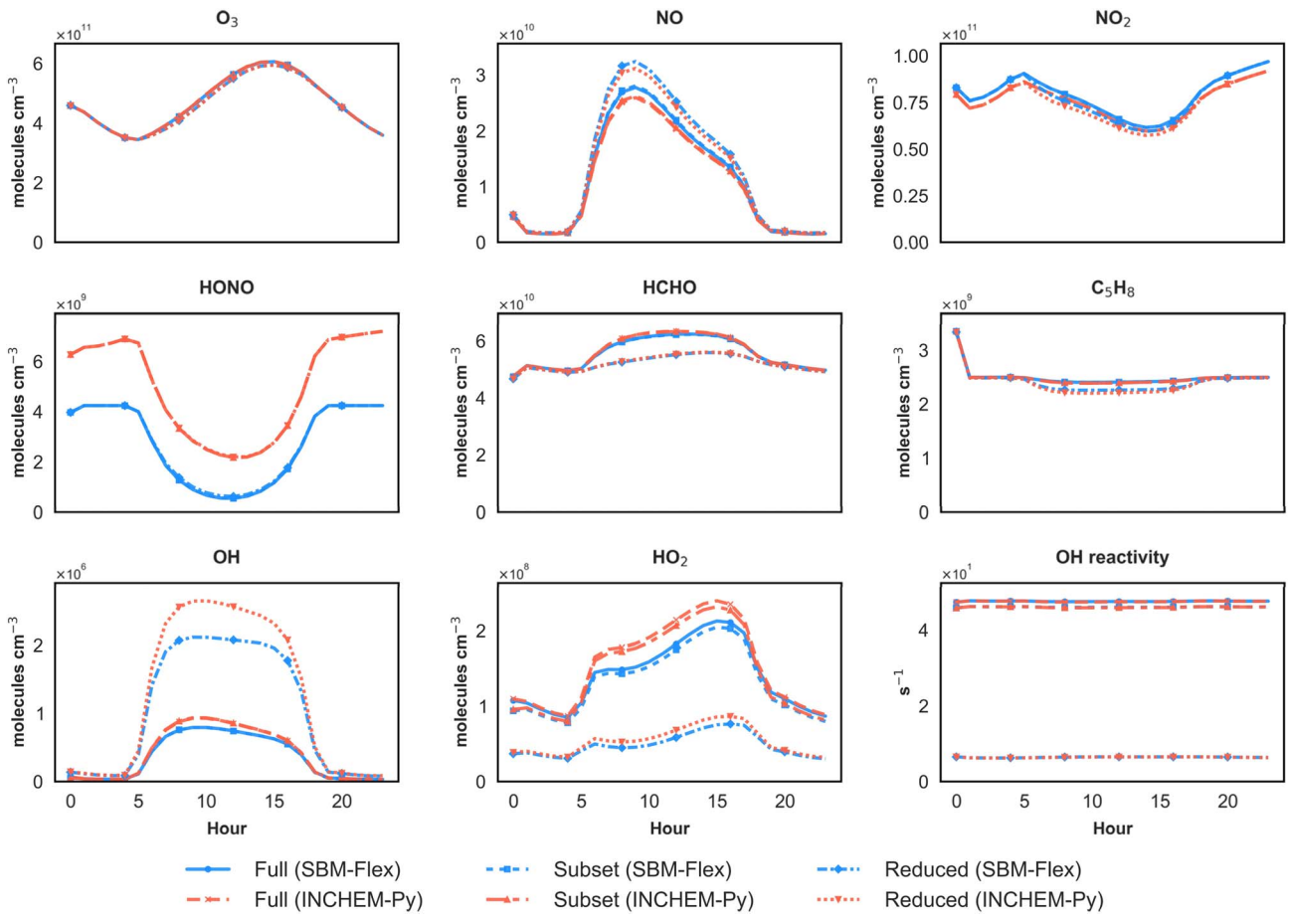

Fig. 3 Simulated diurnal profiles of key photochemically active species and total OH reactivity using SBM-Flex and INCHEM-Py across different chemical mechanisms.

films are already well developed and the HONO formation efficiency approaches a near-saturated regime. As a result, further increases in RH do not substantially enhance HONO production, while reductions to unrealistically low RH values primarily affect conditions outside those observed in this study.

These results indicate that, under the conditions examined here, indoor radical chemistry is relatively insensitive to short-term RH variability, despite the explicit humidity dependence implemented in the HONO formation scheme. Importantly, this behaviour does not imply that humidity is unimportant for indoor HONO formation more generally, but rather that the specific kitchen environment studied here operated within a humidity regime where HONO yields were already constrained by surface water availability. This analysis therefore serves to demonstrate the internal consistency and stability of the revised HONO parameterisation within the observed environmental range, rather than to provide a direct evaluation against HONO or radical measurements, which were not available for this campaign.

In addition, NO_2 measurements may be affected by interference from HONO under indoor conditions, which adds uncertainty to the interpretation of simulated NO_2 differences between model configurations.[60,61]

Moreover, the performance differences across Full, Subset, and Reduced mechanisms provide further insights into the role of chemical complexity in capturing indoor photochemistry. The Subset mechanism closely reproduces the Full mechanism across all species, confirming that the reduced species set retains sufficient complexity to represent key radical propagation and VOC oxidation processes. In contrast, the Reduced mechanism exhibits distinct biases. It predicts higher OH concentrations, due to its oversimplified VOC oxidation scheme, which reduces OH consumption pathways. Conversely, it underestimates HO_2, because its streamlined chemistry omits many secondary radical regeneration steps present in the Full and Subset mechanisms. These differences extend to other key species. Formaldehyde, a major oxidation intermediate, and isoprene, a highly reactive VOC, both show lower concentrations in the reduced mechanism, reflecting the exclusion of key VOC oxidation pathways and intermediates, which limits secondary product formation and reduces OH consumption. Total OH reactivity—a cumulative indicator of the oxidative burden posed by all reactive species—also drops substantially in the Reduced mechanism, consistent with its truncated species set.

3.3 Base case simulation and mechanism comparison

Fig. 4(a) presents the base case simulation results from SBM-Flex for 17 August 2023, comparing indoor concentrations simulated using the Full, Subset, Reduced, and Mini mechanisms against observations. These simulations exclude indoor emissions or occupancy-related effects associated with cooking or cleaning events, thereby representing a low-emission baseline condition. All SBM-Flex mechanisms successfully reproduced indoor concentrations across all air pollutants under the base case, highlighting the model's effectiveness in capturing indoor background conditions. This agreement reflects the model's capability to simulate outdoor-to-indoor transport, baseline indoor photochemistry, and deposition processes under constrained outdoor inputs. Fig. 4(b) shows the corresponding outdoor concentrations used as boundary conditions for the base case simulation.

For outdoor O_3, NO, and NO_2, fitted diurnal profiles derived directly from hourly ambient observations were used as boundary conditions, providing realistic time-resolved inputs for the simulation. This observational constraint ensures that the outdoor chemical variability, particularly important for species with strong photochemical behaviour, are physically well represented in the model. The close agreement between observed and simulated indoor concentrations for these species (Fig. 4(a)) confirms the value of incorporating temporally resolved, observation-based inputs. Direct diurnal fitting was not feasible for other air pollutants due to the lack of a consistent diurnal pattern in the ambient measurements. Instead, daily average concentrations derived from the same observational dataset, presented in Fig. 2, were applied as fixed boundary conditions as the outdoor base case, shown in Fig. 4(b). These values remained constant throughout the simulation, consistent with the treatment employed in INCHEM-Py. As Fig. 4(b) illustrates, the prescribed daily averages effectively capture the overall background levels of the outdoor pollutants.

While the simulation reproduces the overall indoor concentration levels reasonably well, some underestimation is evident for many gas-phase species. This is largely due to the absence of real-time activity inputs or sustained indoor sources in the base case setup. Although observed indoor concentrations were used to initialise the model, no additional emissions were included beyond that point. As a result, the simulated indoor levels tend to gradually stabilise and closely follow the outdoor boundary conditions through ventilation-driven exchange. This behaviour leads to relatively flat concentration profiles over time and contributes to the lower simulated values compared to the measured indoor concentrations, which consistently exceed that outdoors. The observed indoor enhancement suggests that ongoing low-level indoor emissions or dynamic processes, likely present in the real environment, play a role in maintaining elevated concentrations, consistent with previous observations of continuous emissions from building materials and furnishings sustaining elevated indoor VOC baselines even under ventilated conditions.[62]

Since these were not captured in the base case configuration, the model naturally leans towards a more conservative prediction. The underestimation of VOCs, particularly in the case of C_5H_8, may be a result of fragmentation of other compounds to this mass in the PTR-ToF-MS.[63] have shown that other compounds (aldehydes and cycloalkanes) commonly present in indoor environments also contribute to this mass resulting in an overestimate of isoprene concentrations. Such interferences may therefore contribute to the measurement-model discrepancies observed for individual VOC species (*e.g.* Fig. 4), without affecting the interpretation of overall VOC dynamics discussed here.

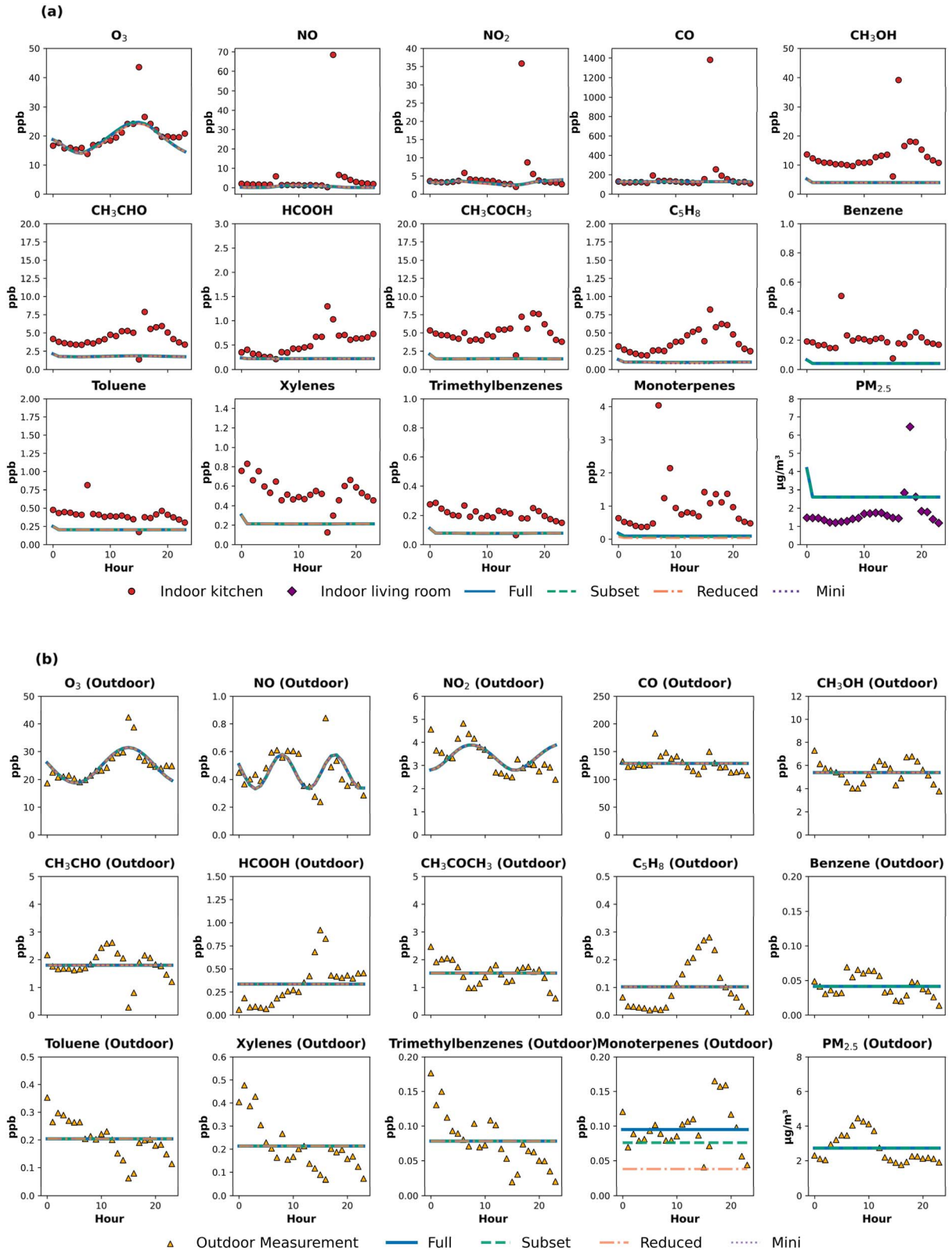

Fig. 4 Diurnal profiles simulation of indoor and outdoor pollutant mixing ratios/concentrations under base case conditions (excluding additional emissions or occupancy effects during cooking and cleaning events) using MBM-Flex (a) Indoor base case simulations using the Full, Subset, Reduced, and Mini mechanisms compared with observations. ($PM_{2.5}$ was measured in the adjacent living room, while gas-phase species were measured in the kitchen) (b) outdoor base case prescribed from observations, with diurnal profiles applied for O_3, NO, and NO_2, and daily averages for other species.

Beyond uncertainties related to emission representation and instrumental artefacts, the treatment of VOC speciation within the model introduces further uncertainty in the simulation of individual compounds. Due to the limited isomer resolution of real-time PTR-ToF-MS measurements, VOC classes were mapped onto the chemical mechanism using an equal-split assumption. While this simplification may influence isomer-specific reaction pathways and the formation of certain secondary products, previous indoor air chemistry modelling studies using similar chemical mechanisms and observational constraints have shown that bulk oxidative behaviour, including overall VOC reactivity, radical budgets, and oxidant responses, is relatively insensitive to the precise isomeric distribution when compound-specific product yields are not the primary focus.[57,64] In the present study, the emphasis is on reproducing overall pollutant dynamics and event-scale behaviour rather than resolving detailed isomer-specific chemistry.

In addition to the overall underestimation of VOCs, the model also predicts a marked decline in both VOC and $PM_{2.5}$ concentrations during the first hour of simulation. For VOCs, this pattern reflects relatively high initial concentrations derived from observations, while for $PM_{2.5}$, the elevated starting values arise from a combination of observational inputs and model-internal contributions, particularly seed aerosol mass. Under base case conditions with no ongoing indoor emissions, both VOCs and $PM_{2.5}$ are rapidly removed *via* chemical transformation, ventilation-driven dilution, and particle deposition. This behaviour is clearly illustrated in Fig. S4, which presents high-frequency model output at 150-seconds resolution. The sharp and simultaneous decline of VOCs and $PM_{2.5}$ suggests that the initial high PM is not actively formed through VOC oxidation, but instead reflects the pre-existing material, followed by the removal process. While the model captures this early depletion well, it consistently overestimates $PM_{2.5}$ concentrations relative to measurements, likely due to overestimated initial seed loading and simplified treatment of particle-phase loss rather than excessive SOA production.

Fig. 4(a) further compares indoor simulation results using the Full, Subset, Reduced, and Mini chemical mechanisms under base case conditions. Across most species, all four mechanisms yield closely overlapping results and effectively reproduce the observed indoor concentrations, demonstrating that background indoor air quality is well captured even with simplified chemistry. In terms of computational demand, the Subset mechanism reduces simulation time by approximately 70% compared to the Full mechanism. The Reduced and Mini schemes further cut runtimes by over 95%.

The differences between mechanisms arise primarily from variations in pollutant representation and the complexity of chemical reactions. The Full mechanism retains the complete set of measured VOCs and $PM_{2.5}$, including all oxygenates, aromatics, and monoterpenes. The Subset mechanism is nearly identical, except for the omission of β-pinene among the monoterpenes. The Reduced mechanism excludes several key pollutants, including $PM_{2.5}$, benzene, and retains only carene and camphene among the monoterpenes. The Mini mechanism is a further simplification, omitting additional compounds such as CH_3COCH_3, toluene, the xylenes, the trimethylbenzenes, and all monoterpenes entirely. As a result, these progressive reductions lead to underrepresentation of several VOCs and particle-phase species in the more simplified schemes due to missing precursors and simplified degradation pathways. This reduction in chemical complexity is especially apparent for monoterpenes, with a stepwise reduction in concentrations from Full to Mini, as seen in Fig. 4(a) and (b).

Among the four mechanisms, the Subset mechanism consistently tracks the Full mechanism most closely across all species, confirming that this simplified alternative retains sufficient chemical complexity to accurately represent the key processes governing indoor air quality under base case conditions.

3.4 Model evaluation during cooking and cleaning events

Based on the strong performance of the Subset mechanism demonstrated in the base case evaluation (Section 3.3), this mechanism was selected for simulating time-resolved pollutant concentrations during the two key events: the morning and afternoon cooking and cleaning periods. Fig. 5 compares measured and simulated concentrations for nine key species during these events, under three configurations: (i) the base case without any additional emissions, (ii) a scenario with event-specific emissions added, and (iii) a scenario with both emissions and enhanced deposition representing human presence. The morning event (Fig. 5(a)) corresponds to cooking starting at 06:00, while the afternoon event (Fig. 5(b)) begins at 16:00, consistent with volunteer activity logs.

Eight species were selected to assess how well the model captures pollutant changes during cooking and cleaning events, including O_3, NO, NO_2, CO, monoterpenes, CH_3CHO, C_5H_8, and CH_3COCH_3. This selection reflects their relevance to cooking and cleaning processes, covering directly emitted species (NO, NO_2, CO, monoterpenes), photochemically reactive species (O_3, C_5H_8), and intermediate oxidation products (CH_3CHO, CH_3COCH_3). In these event simulations, emissions for key primary pollutants (CO, NO, NO_2, monoterpenes) were directly prescribed during the events. Among the monoterpenes, only limonene was included as a primary emission, on account of its dominance in both cooking vapours and fragranced cleaning products.[22] The emission rates were estimated from observed indoor concentration increases to ensure a realistic representation. For example, the emission rate for NO employed in the model was tuned so that the model reproduced the observed changes in indoor NO concentration, *e.g.*, an increase of about 4 ppb from approximately 1.7 ppb to 5.7 ppb during the morning event. Additionally, emissions were applied only during the logged activity hour and ceased afterwards.

In both events, direct emissions of NO, NO_2, CO, and monoterpenes (represented by limonene) produced sharp peaks during the cooking periods. These were well reproduced by the emission-based simulations, and the rapid post-peak decay further supports the short-lived nature of the emission pulse and its realistic representation in the model.

The emission scenario produces an additional O_3 decrease during the cooking period that closely matches the timing and

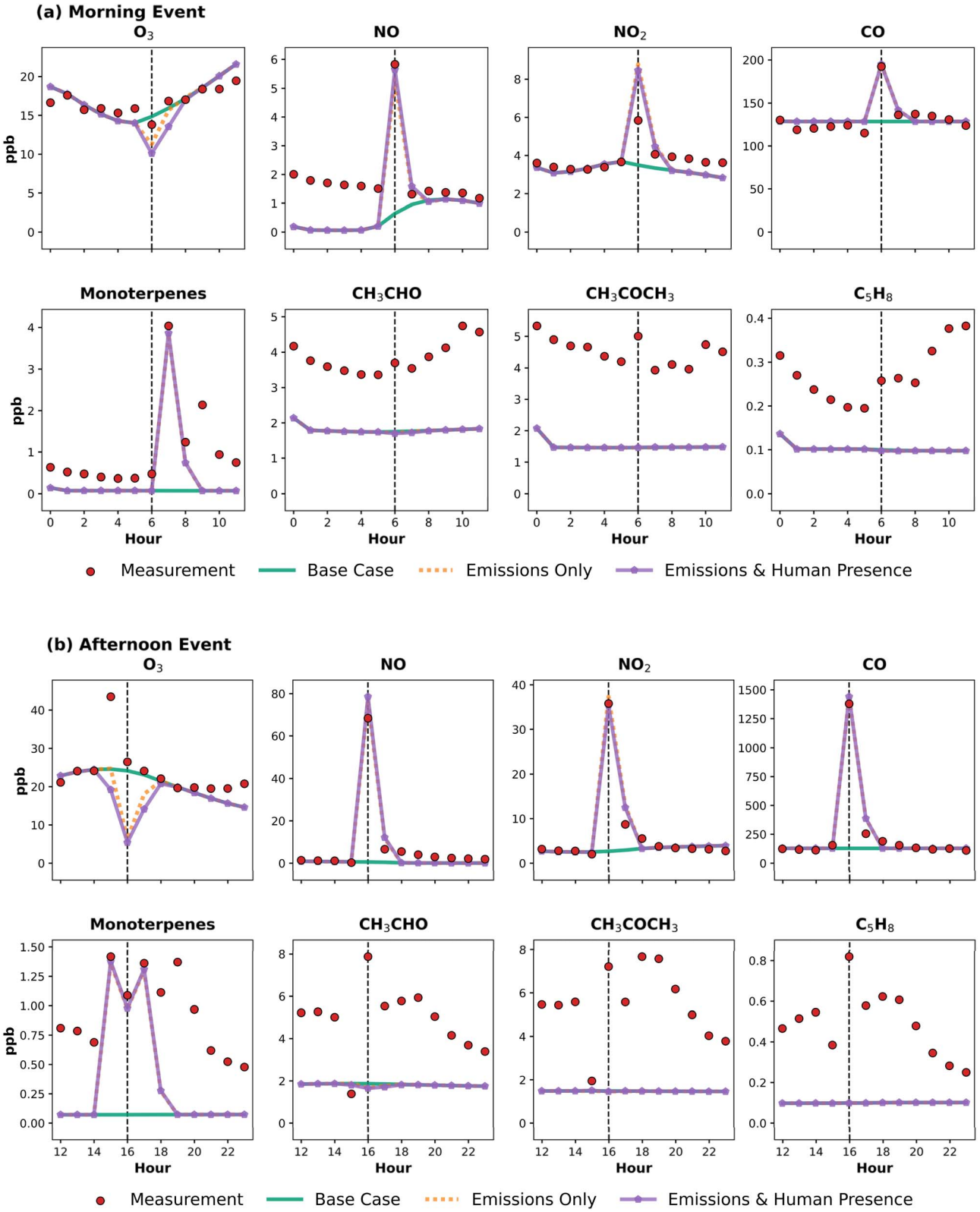

Fig. 5 Comparison of simulated pollutant mixing ratios using Subset mechanism of SBM-Flex under different scenarios—base case (excluding emissions and other occupancy effects during cooking and cleaning events), emissions only, and emissions with human presence—against observations for key species. (a) Morning event (06:00), (b) afternoon event (16:00).

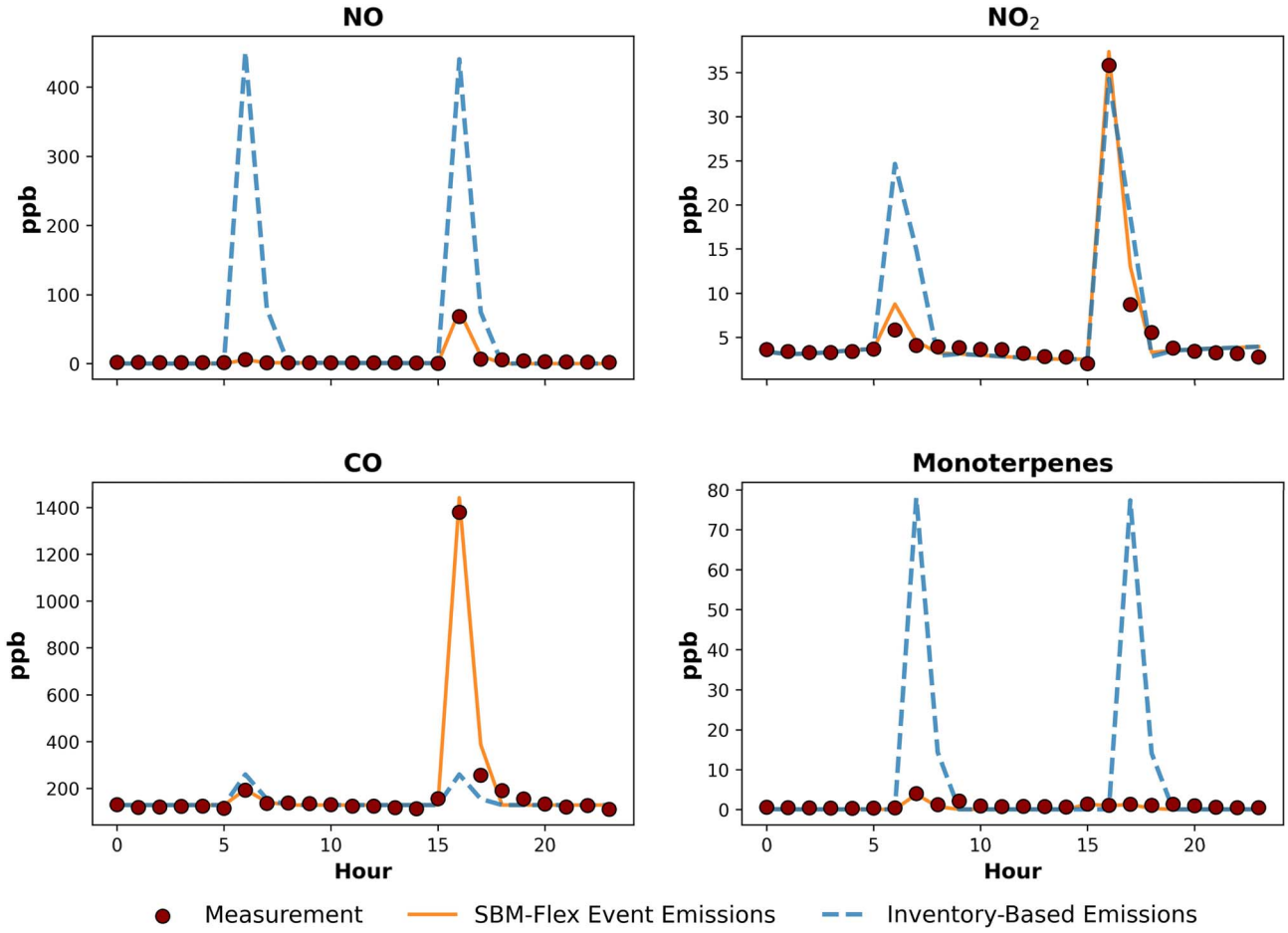

Fig. 6 Comparison of primary pollutant concentrations (NO, NO_2, CO, and monoterpenes) simulated using the SBM-Flex Subset mechanism with event-specific emissions and inventory-based emissions against observations.

magnitude of the observed deviation from expected indoor levels, which will approach outdoor levels due to the ventilation effect. However, at 06:00, indoor O_3 is approximately 6 ppb lower than outdoors, and the emission simulation captures a comparable reduction driven by NO-induced loss. While modelled indoor concentrations remain below observations, primarily because the base case starts from a lower baseline, the added decline reflects the correct chemical response to primary emissions. This indicates that the reaction kinetics governing O_3 removal are realistically represented, even if the absolute levels are underestimated due to baseline bias.

When human presence is additionally included in the model, *via* enhanced deposition to skin surfaces, O_3 removal is further intensified, resulting in even lower concentrations. This supports the role of humans as dynamic sinks for surface-reactive species like O_3. Notably, this effect was more pronounced in the afternoon, when two adults were present for a longer duration (15:00–17:00), compared to only one adult during the morning event (06:00–07:00). In contrast to O_3, monoterpenes showed minimal sensitivity to human presence. While emission-driven peaks were accurately captured, adding human presence had a negligible additional impact, consistent with their weaker surface reactivity. This suggests that direct emissions dominate indoor concentration dynamics during events for monoterpenes, with limited contribution from deposition-related losses.

For VOCs such as CH_3CHO, and C_5H_8, the model shows little or no response to the cooking events, with concentrations closely tracking the base case. This reflects the absence of direct emission inputs for these species in the event simulations. As a result, their behaviour is not well reproduced, and the model fails to capture the observed event-related peaks. A slight decrease relative to the base case is seen during the cooking periods, particularly for CH_3CHO. This likely arises from changes in the indoor chemical environment caused by co-emitted NO, which suppresses oxidant levels (*e.g.*, O_3 and OH) and reduces the secondary formation of oxygenated VOCs. Such effects would be expected primarily for cooking with combustion-based fuels (*e.g.*, gas) and would be absent or substantially reduced when using electric or induction appliances, where NO_x emissions are minimal. These results highlight that without explicit emission or formation pathways; the model underrepresents the dynamics of semi-volatile and reactive VOCs under event conditions.

3.5 Comparison of measurement-informed and inventory-based emission scenarios

To illustrate the limitations of applying aggregated indoor emission inventories to short-term, household-specific events, we compared the measurement-informed emissions derived in this study (Section 3.4) with standard emission factors from the Indoor Air Pollutants Inventory (InAPI) Tool.[42] This comparison is not intended to evaluate the predictive performance of the inventory for this specific case, but rather to demonstrate how inventory-based emission factors—developed to represent average conditions across diverse residential environments—may diverge from event-scale emissions observed in a real home.

InAPI is a scenario-based inventory developed from an extensive compilation of UK indoor air measurements, converted into hourly emission rates using a chemical mass balance (CMB) approach. It allows users to select specific built environments (*e.g.*, residential), micro-environments (*e.g.*, kitchens), and activity types (*e.g.*, cooking) along with associated pollutants. For this study, emissions of NO, NO_2, CO, and monoterpenes (assumed to be limonene) were extracted using the most relevant combinations to reflect the observed activities. However, the emission factors provided by InAPI are time-averaged and are not designed to reproduce the magnitude or temporal structure of short-lived indoor emission events.

Fig. 6 compares simulated indoor concentrations obtained using inventory-based emission factors with those derived from measurement-informed emissions, alongside the observed concentrations for 17 August 2023. The discrepancies between the two emission approaches vary across species and events. Inventory-based emissions substantially overpredict NO and monoterpenes relative to the measurement-informed case, while CO and NO_2 are underestimated during the afternoon event. Importantly, these differences do not follow a consistent direction across species, indicating that inventory emission factors do not systematically over- or underestimate emissions for this household.

These discrepancies primarily reflect the aggregated nature of emission inventories, which are constructed to represent average conditions across a wide range of residential environments, fuel types, ventilation scenarios, and occupant behaviours. As such, inventory-based emission factors are not expected to reproduce the magnitude or temporal structure of short-term emission events in a specific dwelling, particularly where activities, appliance use, and ventilation differ from inventory assumptions.

This comparison therefore serves as a specific illustration of the limitations of applying generic indoor emission inventories to event-scale modelling in individual homes. While inventory-based emission factors are valuable for long-term exposure assessments and population-level analyses, they may misrepresent short-term indoor pollutant dynamics driven by specific activities and behaviours. In contrast, measurement-informed emissions, despite their own uncertainties, provide a more appropriate representation of short-duration indoor air pollution events when the objective is to reproduce observed concentration dynamics.

4 Conclusions

This study evaluated the performance of the newly developed SBM-Flex model, built upon INCHEM-Py (v1.2), for simulating indoor air pollutant dynamics in a real residential environment. A range of simulation setups was assessed, including a no-emission base case, scenarios with event-specific emissions from cooking and cleaning, configurations incorporating human presence, and comparisons against inventory-based emission estimates. Simulation results were evaluated using reference-grade instruments, supported by a custom-developed auto-valve switching system that enabled time-alternating indoor and outdoor sampling with a single instrument suite, ensuring consistent and high-quality measurements.

The model successfully captured key pollutant behaviours, including peak concentrations of NO, NO_2, CO, and monoterpenes during cooking and cleaning events, as well as O_3 depletion *via* NO reactions and surface deposition. A humidity-dependent HONO parameterisation improved the process-level representation of indoor radical chemistry, while the Subset mechanism demonstrated strong performance in balancing chemical completeness with computational efficiency.

While SBM-Flex performed well overall, several limitations remain. The lack of detailed behavioural records constrained the ability to represent activity-driven pollutant changes, particularly for reactive VOCs. This limitation highlights the importance of detailed and systematic activity logging in future real-world indoor air quality field studies, especially for the quantitative attribution of short-term emission events. The use of daily average outdoor concentrations as boundary conditions for some species limited the model's capacity to reproduce realistic indoor diurnal profiles. Inventory-based emissions, though broadly informative, may not capture short-term or case-specific indoor events. Additionally, the assumption of a well-mixed indoor environment may not align with point-based measurements during transient emission periods. In addition, a dedicated tracer-gas method would have provided a more direct estimate of the air change rate, but such measurements were not available in this study; instead, ACR was constrained indirectly using the available multi-species observations, which may introduce some uncertainty into the ventilation representation.

Despite these limitations, the results demonstrate that SBM-Flex is a robust and versatile tool for characterising indoor air pollutant dynamics under realistic conditions. Its ability to capture both background and event-driven variations, combined with low computational demand, makes it particularly valuable for future applications in exposure assessment, source attribution, and the design of targeted indoor air quality interventions.

Author contributions

YS: carrying out the modelling; data analysis; writing original draft; review & editing of paper; RSommariva: conceptualisation; model development; supervising the modelling; review & editing of paper; JL: conceptualisation; initial model

development in particular for use of multiple model boxes representing multiple rooms; initial supervision of RSommariva; review of paper; RSahu: carrying out the field measurements; AM: providing input on indoor emissions inventory comparison; review of paper; JB: evaluation of measurement data except for VOCs; review of paper; JA: evaluation of VOC measurement data; review & editing of paper; DRS: implementation of changes to INCHEM-Py and advice on INCHEM-Py; ZS: day-to-day supervision of RSahu and contributions to measurement campaign; review of paper; WB: supervision of chemical scheme intercomparison and supervision of RSommariva during this period; review of paper; ZN: providing input on indoor emissions inventory comparison; review of paper; CP: conceptualisation; lead of overall project and supervision of RSommariva and YS; key inputs on indoor emissions inventory and model developments; review & editing of paper.

Conflicts of interest

The authors confirm that there are no conflicts of interest to declare.

Data availability

The original measurement data used to validate the model presented in this article, including metadata are available (embargoed until 1st April 2027) at UBIRA eData at https://edata.bham.ac.uk/1264/. The data supporting this article have been included as part of the supplementary information (SI). Further details are available from the corresponding author upon request. Latest model code developments will be made available at https://github.com/IndoorAir together with related indoor air research; the latest box model code is available at https://github.com/IndoorAir/MBM-Flex. Supplementary information: complementary tables and figures on model conditions, statistical evaluation of the model-measurement comparison, air change rate (ACR) optimisation as well as further modelling and measurement details. See DOI: https://doi.org/10.1039/d5em00987a.

Acknowledgements

We are very grateful for input and indirect contributions from the IAQ-EMS co-investigators Suzanne Bartington, Zhiwen Luo, Bruno Fraga, Zhen Liu and Hassan Hemida. Nicola Carslaw is acknowledged for collaborative input and help with interfacing the INCHEM-Py model[35] with a range of chemical schemes in particular. This project is funded through the MetOffice/Strategic Priorities' Fund (SPF) research grant "Indoor Air Quality Emissions & Modelling System (IAQ-EMS)". Support was also received through Natural Environment Research Council (NERC)/SPF grant "Air Pollution Solutions for Vulnerable Groups (CleanAir4V)" and observations benefitted also from NERC grant (NE/V017624/1).

References

1 S. Dimitroulopoulou, M. R. Dudzinska, L. Gunnarsen, L. Hagerhed, H. Maula, R. Singh, *et al.*, Indoor air quality guidelines from across the world: An appraisal considering energy saving, health, productivity, and comfort, *Environ. Int.*, 2023, **178**, 108127.
2 S. Uchiyama, M. Noguchi, M. Hishiki, M. Shimizu, N. Kunugita, T. Isobe, *et al.*, Long-term monitoring of indoor, outdoor, and personal exposure to gaseous chemical compounds, *Sci. Total Environ.*, 2024, **906**, 167830.
3 WHO.7 Million Premature Deaths Annually Linked to Air Pollution News Release on 25 March 2014 at.
4 I. Kang, A. McCreery, P. Azimi, A. Gramigna, G. Baca, K. Abromitis, *et al.*, Indoor air quality impacts of residential mechanical ventilation system retrofits in existing homes in Chicago, IL, *Sci. Total Environ.*, 2022, **804**, 150129.
5 M. Mannan and S. G. Al-Ghamdi, Indoor Air Quality in Buildings: A Comprehensive Review on the Factors Influencing Air Pollution in Residential and Commercial Structure, *Int. J. Environ. Res. Public Health*, 2021, **18**(6), 3276.
6 W. W. Nazaroff and C. J. Weschler, Indoor ozone: Concentrations and influencing factors, *Indoor Air*, 2022, **32**(1), e12942.
7 J. Gonzalez-Martin, N. J. R. Kraakman, C. Perez, R. Lebrero and R. Munoz, A state-of-the-art review on indoor air pollution and strategies for indoor air pollution control, *Chemosphere*, 2021, **262**, 128376.
8 B. You, W. Zhou, J. Li, Z. Li and Y. Sun, A review of indoor Gaseous organic compounds and human chemical Exposure: Insights from Real-time measurements, *Environ. Int.*, 2022, **170**, 107611.
9 E. D. Lebel, C. J. Finnegan, Z. Ouyang and R. B. Jackson, Methane and NO(x) Emissions from Natural Gas Stoves, Cooktops, and Ovens in Residential Homes, *Environ. Sci. Technol.*, 2022, **56**(4), 2529–2539.
10 P. J. Irga, G. Mullen, R. Fleck, S. Matheson, S. J. Wilkinson and F. R. Torpy, Volatile organic compounds emitted by humans indoors– A review on the measurement, test conditions, and analysis techniques, *Build. Sci.*, 2024, 255.
11 N. Carslaw, L. Fletcher, D. Heard, T. Ingham and H. Walker, Significant OH production under surface cleaning and air cleaning conditions: Impact on indoor air quality, *Indoor Air*, 2017, **27**(6), 1091–1100.
12 J. C. Ditto, L. R. Crilley, M. Lao, T. C. VandenBoer, J. P. D. Abbatt and A. W. H. Chan, Indoor and outdoor air quality impacts of cooking and cleaning emissions from a commercial kitchen, *Environ. Sci.:Processes Impacts*, 2023, **25**(5), 964–979.
13 R. E. Militello-Hourigan and S. L. Miller, The impacts of cooking and an assessment of indoor air quality in Colorado passive and tightly constructed homes, *Build. Sci.*, 2018, **144**, 573–582.
14 R. Tang and C. Pfrang, Indoor particulate matter (PM) from cooking in UK students' studio flats and associated

intervention strategies: evaluation of cooking methods, PM concentrations and personal exposures using low-cost sensors, *Environ. Sci.: Atmos.*, 2023, **3**(3), 537–551.
15 Y. Su, Y. Dai, Z. Shi, Y. Jiang, L. Kong and C. Pfrang, Natural Ventilation Reduces Cooking-Related PM2.5 Peaks Indoors, *ACS ES&T Air*, 2026, **3**(2), 590–599.
16 R. Tang, Y. Su, W. J. F. Acton, L. K. Dunn and C. Pfrang, Quantification of Volatile Organic Compounds (VOCs), Nitrogen Oxides (NO_x), and Ultrafine Particles (UFPs) Emitted by Domestic Air Fryers: A Chamber Study of Indoor Air Quality Impacts, *ACS ES&T Air*, 2026, **3**(2), 473–487.
17 R. Tang, B. Yu and C. Pfrang, Cooking aerosols in all-electric flat and studio accommodations: event-scale emissions, transport, and exposure assessments using low-cost sensors, *Environ. Sci.:Adv.*, 2026, DOI: 10.1039/D5VA00442J.
18 T. Liu, Z. Wang, X. Wang and C. K. Chan, Primary and secondary organic aerosol from heated cooking oil emissions, *Atmos. Chem. Phys.*, 2018, **18**(15), 11363–11374.
19 P. Kumar, A. B. Singh, T. Arora, S. Singh and R. Singh, Critical review on emerging health effects associated with the indoor air quality and its sustainable management, *Sci. Total Environ.*, 2023, **872**, 162163.
20 F. Klein, U. Baltensperger, A. S. H. Prevot and I. El Haddad, Quantification of the impact of cooking processes on indoor concentrations of volatile organic species and primary and secondary organic aerosols, *Indoor Air*, 2019, **29**(6), 926–942.
21 D. A. Jaffe and A. Creekmore, Emissions and exposure to NOx, CO, CO2 and PM2.5 from a gas stove using reference and low-cost sensors, *Atmos. Environ.*, 2024, **331**, 120564.
22 D. Campagnolo, D. E. Saraga, A. Cattaneo, A. Spinazzè, C. Mandin, R. Mabilia, *et al.*, VOCs and aldehydes source identification in European office buildings - The OFFICAIR study, *Build. Sci.*, 2017, **115**, 18–24.
23 Y. W. Kim, M. J. Kim, B. Y. Chung, Y. Bang du, S. K. Lim, S. M. Choi, *et al.*, Safety evaluation and risk assessment of d-Limonene, *J. Toxicol. Environ. Health B Crit. Rev.*, 2013, **16**(1), 17–38.
24 A. Luengas, A. Barona, C. Hort, G. Gallastegui, V. Platel and A. Elias, A review of indoor air treatment technologies, *Rev. Environ. Sci. Bio/Technol.*, 2015, **14**(3), 499–522.
25 W. W. Nazaroff and C. J. Weschler, Methanol and ethanol in indoor environments, *Indoor Environ.*, 2024, **1**(4), 100049.
26 R. Tang, R. Sahu, Y. Su, A. Milsom, A. Mishra, T. Berkemeier, *et al.*, Impact of Cooking Methods on Indoor Air Quality: A Comparative Study of Particulate Matter (PM) and Volatile Organic Compound (VOC) Emissions, *Indoor Air*, 2024, **2024**(1), 6355613.
27 T. Z. Maung, R. Aning, M. Newnham, E. Holt, C. Pfrang and A. M. Turner, Indoor air quality and its impacts on asthma and COPD, *BMJ Open Respir. Res.*, 2026, **13**(1), e003807.
28 T. Z. Maung, J. E. Bishop, E. Holt, A. M. Turner and C. Pfrang, Indoor Air Pollution and the Health of Vulnerable Groups: A Systematic Review Focused on Particulate Matter (PM), Volatile Organic Compounds (VOCs) and Their Effects on Children and People with Pre-Existing Lung Disease, *Int. J. Environ. Res. Public Health*, 2022, **19**(14), 8752.
29 J. P. D. Abbatt and C. Wang, The atmospheric chemistry of indoor environments, *Environ. Sci.:Processes Impacts*, 2020, **22**(1), 25–48.
30 S. Gligorovski and C. J. Weschler, The oxidative capacity of indoor atmospheres, *Environ. Sci. Technol.*, 2013, **47**(24), 13905–13906.
31 J. Liu, S. Li, J. Zeng, M. Mekic, Z. Yu, W. Zhou, *et al.*, Assessing indoor gas phase oxidation capacity through real-time measurements of HONO and NO(x) in Guangzhou, China, *Environ. Sci.:Processes Impacts*, 2019, **21**(8), 1393–1402.
32 M. Mendez, N. Blond, D. Amedro, D. A. Hauglustaine, P. Blondeau, C. Afif, *et al.*, Assessment of indoor HONO formation mechanisms based on *in situ* measurements and modeling, *Indoor Air*, 2017, **27**(2), 443–451.
33 S. P. O'Meara, S. Xu, D. Topping, M. R. Alfarra, G. Capes, D. Lowe, *et al.*, PyCHAM (v2.1.1): a Python box model for simulating aerosol chambers, *Geosci. Model Dev.*, 2021, **14**(2), 675–702.
34 D. K. Farmer, M. E. Vance, J. P. D. Abbatt, A. Abeleira, M. R. Alves, C. Arata, *et al.*, Overview of HOMEChem: House Observations of Microbial and Environmental Chemistry, *Environ. Sci.:Processes Impacts*, 2019, **21**(8), 1280–1300.
35 D. R. Shaw, T. J. Carter, H. L. Davies, E. Harding-Smith, E. C. Crocker, G. Beel, *et al.*, INCHEM-Py v1.2: a community box model for indoor air chemistry, *Geosci. Model Dev.*, 2023, **16**(24), 7411–7431.
36 F. F. Osterstrom, T. J. Carter, D. R. Shaw, J. P. D. Abbatt, A. Abeleira, C. Arata, *et al.*, Modelling indoor radical chemistry during the HOMEChem campaign, *Environ. Sci.:Processes Impacts*, 2025, **27**(1), 188–201.
37 D. R. Shaw, *INCHEM-Py 2023*, https://github.com/DrDaveShaw/INCHEM-Py.
38 Z. Liu, C. Pfrang, R. Sommariva, J. Brean, Y. Su, W. Bloss, *et al.*, A coupled fluids-chemistry model for pollutant dynamics indoors—Application to a kitchen scenario, *Phys. Fluids*, 2025, **37**(5), 053336.
39 P. S. J. Lakey, Y. Won, D. Shaw, F. F. Osterstrom, J. Mattila, E. Reidy, *et al.*, Spatial and temporal scales of variability for indoor air constituents, *Commun. Chem.*, 2021, **4**(1), 110.
40 S. M. Saunders, M. E. Jenkin, R. G. Derwent and M. J. Pilling, Protocol for the development of the Master Chemical Mechanism, MCM v3 (Part A): tropospheric degradation of non-aromatic volatile organic compounds, *Atmos. Chem. Phys.*, 2003, **3**(1), 161–180.
41 M. E. Jenkin, S. M. Saunders, V. Wagner and M. J. Pilling, Protocol for the development of the Master Chemical Mechanism, MCM v3 (Part B): tropospheric degradation of aromatic volatile organic compounds, *Atmos. Chem. Phys.*, 2003, **3**(1), 181–193.
42 A. Mazzeo, C. Pfrang and Z. A. Nasir, InAPI (v1.0): an Excel-based Indoor Air Pollution Inventory tool to visualise activity-based indoor concentrations of pollutants and their emission rates for the UK, *EGUsphere*, 2025, 1–14.

43 M. Shiraiwa, N. Carslaw, D. J. Tobias, M. S. Waring, D. Rim, G. Morrison, *et al.*, Modelling consortium for chemistry of indoor environments (MOCCIE): integrating chemical processes from molecular to room scales, *Environ. Sci.:Processes Impacts*, 2019, **21**(8), 1240–1254.

44 England PH, *Indoor Air Quality Guidelines for Selected Volatile Organic Compounds (VOCs) in the UK*. Public Heath England, London, UK, 2019.

45 R. Taipale, T. M. Ruuskanen, J. Rinne, M. K. Kajos, H. Hakola, T. Pohja, *et al*, Technical Note: Quantitative long-term measurements of VOC concentrations by PTR-MS – measurement, calibration, and volume mixing ratio calculation methods, *Atmos. Chem. Phys.*, 2008, **8**(22), 6681–6698.

46 J. Li, A. C. Lewis, J. R. Hopkins, S. J. Andrews, T. Murrells, N. Passant, *et al.*, The impact of multi-decadal changes in VOC speciation on urban ozone chemistry: a case study in Birmingham, United Kingdom, *Atmos. Chem. Phys.*, 2024, **24**(10), 6219–6231.

47 N. Carslaw, A new detailed chemical model for indoor air pollution, *Atmos. Environ.*, 2007, **41**(6), 1164–1179.

48 V. B. Bright, W. J. Bloss and X. Cai, Urban street canyons: Coupling dynamics, chemistry and within-canyon chemical processing of emissions, *Atmos. Environ.*, 2013, **68**, 127–142.

49 B. C. McDonald, J. A. De Gouw, J. B. Gilman, S. H. Jathar, A. Akherati, C. D. Cappa, *et al.*, Volatile chemical products emerging as largest petrochemical source of urban organic emissions, *Science*, 2018, **359**(6377), 760–764.

50 B. Yuan, A. R. Koss, C. Warneke, M. Coggon, K. Sekimoto and J. A. de Gouw, Proton-transfer-reaction mass spectrometry: applications in atmospheric sciences, *Chem. Rev.*, 2017, **117**(21), 13187–13229.

51 R. Sommariva, T. S. Bates, D. Bon, D. M. Brookes, J. A. de Gouw, J. B. Gilman, *et al.*, Modelled and measured concentrations of peroxy radicals and nitrate radical in the U.S. Gulf Coast region during TexAQS 2006, *J. Atmos. Chem.*, 2012, **68**(4), 331–362.

52 R. Woodward-Massey, R. Sommariva, L. K. Whalley, D. R. Cryer, T. Ingham, W. J. Bloss, *et al.*, Radical chemistry and ozone production at a UK coastal receptor site, *Atmos. Chem. Phys.*, 2023, **23**(22), 14393–14424.

53 Y. Su, Y. Dai and C. Pfrang, Air exchange rates in a naturally ventilated apartment: a multi-box modelling approach using occupant-generated CO_2 decay measurements, *Res. Eng.*, 2026, **30**, 110563.

54 P. S. Monks, C. Granier, S. Fuzzi, A. Stohl, M. L. Williams, H. Akimoto, *et al.*, Atmospheric composition change – global and regional air quality, *Atmos. Environ.*, 2009, **43**(33), 5268–5350.

55 J. H. Seinfeld and S. N. Pandis, *Atmospheric Chemistry and Physics: from Air Pollution to Climate Change*: John Wiley & Sons, 2016.

56 M. S. Angulo, M. Verriele, M. Nicolas and F. Thevenet, Indoor use of essential oil-based cleaning products: Emission rate and indoor air quality impact assessment based on a realistic application methodology, *Atmos. Environ.*, 2021, 246.

57 H. L. Davies, C. O'Leary, T. Dillon, D. R. Shaw, M. Shaw, A. Mehra, *et al.*, A measurement and modelling investigation of the indoor air chemistry following cooking activities, *Environ. Sci.:Processes Impacts*, 2023, **25**(9), 1532–1548.

58 H. Liu, C. Fang, J. Zhao, Q. Zhou, Y. Dong and L. Lin, The detection of acetone in exhaled breath using gas Pre-Concentrator by modified Metal–Organic framework nanoparticles, *Chem. Eng. J.*, 2024, **498**, 155309.

59 B. J. Finlayson-Pitts, L. M. Wingen, A. L. Sumner, D. Syomin and K. A. Ramazan, The heterogeneous hydrolysis of NO_2 in laboratory systems and in outdoor and indoor atmospheres: An integrated mechanism, *Phys. Chem. Chem. Phys.*, 2003, **5**(2), 223–242.

60 M. S. Alam, L. R. Crilley, J. D. Lee, L. J. Kramer, C. Pfrang, M. Vázquez-Moreno, *et al.*, Interference from alkenes in chemiluminescent NOx measurements, *Atmos. Meas. Tech.*, 2020, **13**(11), 5977–5991.

61 S. Zhou, C. J. Young, T. C. VandenBoer, S. F. Kowal and T. F. Kahan, Time-Resolved Measurements of Nitric Oxide, Nitrogen Dioxide, and Nitrous Acid in an Occupied New York Home, *Environ. Sci. Technol.*, 2018, **52**(15), 8355–8364.

62 Y. Liu, P. K. Misztal, J. Xiong, Y. Tian, C. Arata, R. J. Weber, *et al.*, Characterizing sources and emissions of volatile organic compounds in a northern California residence using space- and time-resolved measurements, *Indoor Air*, 2019, **29**(4), 630–644.

63 L. Ernle, N. Wang, G. Bekö, G. Morrison, P. Wargocki, C. J. Weschler, *et al.*, Assessment of aldehyde contributions to PTR-MS m/z 69.07 in indoor air measurements, *Environ. Sci.: Atmos.*, 2023, **3**(9), 1286–1295.

64 T. J. Carter, D. G. Poppendieck, D. Shaw and N. Carslaw, A Modelling Study of Indoor Air Chemistry: The Surface Interactions of Ozone and Hydrogen Peroxide, *Atmos. Environ.*, 2023, 297.